

BUCKLING ANALYSIS OF SHORT CARBON NANOTUBES BASED ON A NOVEL TIMOSHENKO BEAM MODEL

REZA HOSSEINI-ARA, HAMID R. MIRDAADI, HASAN KHADEMYZADEH

Isfahan University of Technology, Department of Mechanical Engineering, Isfahan, Iran

e-mail: r.hosseiniara@me.iut.ac.ir

In this paper, we present a novel method to investigate the buckling behavior of short clamped carbon nanotubes (CNTs) with small-scale effects. Based on the nonlocal Timoshenko beam kinematics, the strain gradient theory and variational methods, the higher-order governing equation and its corresponding boundary conditions are derived, which are often not considered. Then, we solve the governing differential equation and determine exact critical buckling loads using a linear polynomial plus trigonometric functions different from the purely trigonometric series. We also investigate the influences of the scale coefficients, aspect ratio and transverse shear deformation on the buckling of short clamped CNTs. Moreover, we compare the critical strains with the results obtained from the Sanders shell theory and validate them with molecular dynamic simulations which are found to be in good agreement. The results show that unlike the other beam theories, this model can capture correctly the small-scale effects on buckling strains of short CNTs for the shell-type buckling.

Key words: short carbon nanotubes, buckling, nonlocal elasticity, Timoshenko beam theory

1. Introduction

Since discovering carbon nanotubes (CNTs) by Iijima (1991) more than a decade ago, scientists have been exploring possible uses for carbon nanotubes, which exhibit superior electrical, chemical and mechanical properties. Owing to these properties, CNTs can be applied as nano-probes, nano-needles, reinforcing fibers in composites, nano-actuators, nano-vessels for hydrogen storage and gene delivery systems and nanoscale electronic devices in nano-electromechanical systems (Zhang *et al.*, 2009; Wang *et al.*, 2010).

Meanwhile, the application of short CNTs has prompted significant effort to reduce the size of these nanoscale devices. Seidel *et al.*, (2005) showed that short CNTs, with lengths less than 20 nanometers, are useful in molecular electronics and CNT field-effect transistors (CNTFETs). In addition, they are smaller than many large proteins in the bloodstream, so tubes of that length could find uses as biomedical sensors.

As a result, the importance of carbon nanotubes is realized and both theoretical and experimental works are carried out (Muc, 2011; Yakobson *et al.*, 1996). One property in particular that has been extensively studied is the buckling of single-walled carbon nanotubes (SWCNTs) under axial compression. In fact, nanotubes are highly susceptible to buckling under compression, which is a structural instability. Once the buckling of CNTs occurs, the load-carrying capability would suddenly reduce and lead to possible catastrophic failure of the nanotubes, which can significantly limit the loading strengths of the probing tips and compressive strengths of nanocomposites. Even the physical properties such as conductance of a carbon nanotube can be influenced by the occurrence of buckling (Postma *et al.* 2001). Hence, it is crucial to understand the mechanism of nanotube buckling and even predict the onset of buckling in order to improve the nanotube applications.

To this end, continuum mechanical modeling methods and Molecular dynamics (MD) simulations therefore play important roles in investigating the key characters of the structural and mechanical properties of CNTs. Yakobson *et al.* (1996) conducted some of the early studies that explored the buckling behavior of SWCNTs under various conditions including bending, compression, and twisting. They proposed that classical mechanics can be employed to predict the buckling strain of SWCNTs under strain based upon certain approximations. However, at atomic length scale, the material microstructure becomes increasingly important and small-scale effects cannot be ignored. In order to improve the CNT constitutive relations, many authors adopted Eringen's equations of nonlocal elasticity introduced by Eringen and Edelen (1972) and Eringen (1972, 1976, 1983, 2002), and incorporated them into several continuum models (Feliciano *et al.*, 2011; Kumar *et al.*, 2008; Lu *et al.*, 2006; Peddieson *et al.*, 2003; Reddy, 2007; Reddy and Pang, 2008; Sudak, 2003; Wang B. *et al.*, 2010; Wang C.M., *et al.*, 2007; Wang Q. *et al.*, 2006; Wang Q., 2005; Wang Q. and Wang C.M., 2007; Wang Y.Z. *et al.*, 2010; Yang *et al.*, 2010; Zhang *et al.*, 2004). The use of nonlocal elasticity relations in either Euler-Bernoulli or Timoshenko beam models were shown to be accurate for the buckling strains of the long CNTs (Silvestre *et al.*, 2011; Zhang *et al.*, 2009).

In addition, for short SWCNTs with large diameters, the nonlocal shell model with the appropriate small length scale parameter can provide critical strains that are in good agreement with MD results (Silvestre *et al.*, 2011). However, for short SWCNTs with small diameters, more work has to be done to refine the nonlocal beam and shell models for better prediction of critical strains (Silvestre *et al.*, 2011).

In this paper, we investigate the use of the more refined Timoshenko beam theory for modeling the buckling behavior of CNTs with small aspect ratios. The nonlocal Timoshenko beam model results are compared with the Sanders thin shell model results and validated against MD simulations results. It will be shown herein that unlike the other beam models, the current Timoshenko beam model can correctly reproduce the buckling strains of short CNTs that are length dependent, and these results are relatively close to those predicted by MD simulations.

2. Nonlocal Timoshenko beam theory

The nonlocal elasticity model was first presented by Eringen (1972). According to this model, the stress at a reference point in the body is dependent not only on the strain state at that point, but also on the strain state at all of the points throughout the body. The constitutive equation of the nonlocal elasticity can be written as follows

$$[1 - (e_0 a)^2 \nabla^2] \sigma_{ij} = C_{ijkl} \varepsilon_{kl} \quad (2.1)$$

where C_{ijkl} is the elastic modulus tensor of the classical isotropic elasticity; and σ_{ij} and ε_{kl} are the stress and strain tensors, respectively. In addition, e_0 is a nondimensional material constant, determined by experiments, and a is an internal characteristic length (e.g., a lattice parameter, granular distance). Therefore, $e_0 a$ is a constant parameter that showing the small-scale effect in nano-structures.

The assumed displacement field of the Timoshenko beam kinematics is

$$u_1(x, y, z, t) = u(x, t) + z\phi(x, t) \quad u_2(x, y, z, t) = 0 \quad u_3(x, y, z, t) = w(x, t) \quad (2.2)$$

where ϕ denotes the rotation of the cross section at the point x about the y -axis. The remaining nonzero axial and transverse shear strains are given by

$$\varepsilon_{xx} = \frac{\partial u}{\partial x} + z \frac{\partial \phi}{\partial x} \quad \gamma \equiv 2\varepsilon_{xz} = \frac{\partial w}{\partial x} + \phi \quad (2.3)$$

Using Eq. (2.1), the nonlocal stress tensor components are

$$\sigma_{xx} - (e_0a)^2 \frac{\partial^2 \sigma_{xx}}{\partial x^2} = E\varepsilon_{xx} \quad \sigma_{xz} - (e_0a)^2 \frac{\partial^2 \sigma_{xz}}{\partial x^2} = K_S G \gamma \quad (2.4)$$

The nonlocal stress resultants of the axial force, shear, and bending moment are derived from the above equations, respectively

$$\begin{aligned} N_{NL} - (e_0a)^2 \frac{\partial^2 N_{NL}}{\partial x^2} &= EA \frac{\partial u}{\partial x} & Q_{NL} - (e_0a)^2 \frac{\partial^2 Q_{NL}}{\partial x^2} &= K_S G A \gamma \\ M_{NL} - (e_0a)^2 \frac{\partial^2 M_{NL}}{\partial x^2} &= EI \frac{\partial \phi}{\partial x} \end{aligned} \quad (2.5)$$

where E , G , A and I are Young's modulus, shear modulus, cross-sectional area of beam and area moment of inertia of the beam cross section, respectively. Additionally, K_S denotes the shear correction factor, defined by

$$Q = K_S \int_A \sigma_{xz} dA \quad (2.6)$$

This factor corrects the assumption of constant shear strain on the cross section of the beam in the Timoshenko model, depending on the material and geometry of the cross section.

3. Strain gradient elasticity

Solving Eq. (2.4), the nonlocal axial and shear stresses as a function of the displacement field can be determined as follows

$$\begin{aligned} \sigma(x, z) &= E \left[\varepsilon(x, z) + (e_0a)^2 \frac{\partial^2 \varepsilon(x, z)}{\partial x^2} + (e_0a)^4 \frac{\partial^4 \varepsilon(x, z)}{\partial x^4} + \dots \right] \\ \tau(x) &= K_S G \left[\gamma(x) + (e_0a)^2 \frac{d^2 \gamma(x)}{dx^2} + (e_0a)^4 \frac{d^4 \gamma(x)}{dx^4} + \dots \right] \end{aligned} \quad (3.1)$$

Assuming $(e_0a)^2 \ll 1$, and neglecting the higher powers of the nonlocal parameter, $(e_0a)^4$, $(e_0a)^6$, etc., the solution could be simplified to

$$\sigma(x, z) = E \left[\varepsilon(x, z) + (e_0a)^2 \frac{\partial^2 \varepsilon(x, z)}{\partial x^2} \right] \quad \tau(x) = K_S G \left[\gamma(x) + (e_0a)^2 \frac{d^2 \gamma(x)}{dx^2} \right] \quad (3.2)$$

In fact, Eqs. (3.2) can be thought of as constituting a strain gradient form of the nonlocal beam model (Peddieson *et al.*, 2003). Considering the strain gradient approach, for a Timoshenko beam subjected to an external compressive and conservative force field N_0 , and laterally distributed load $p(x)$, the total potential energy Π , is given by Kumar *et al.* (2008) is generalized in the presence of shear deformation effects as follows

$$\begin{aligned} \Pi &= \int_V \left[\frac{E\varepsilon^2(x, z)}{2} - (e_0a)^2 \frac{E}{2} \left(\frac{\partial \varepsilon(x, z)}{\partial x} \right)^2 \right] dv + \int_V \left[\frac{K_S G \gamma^2(x)}{2} - (e_0a)^2 \frac{K_S G}{2} \left(\frac{d\gamma(x)}{dx} \right)^2 \right] dv \\ &+ \int_0^L \left(N_0 \frac{du}{dx} \right) dx - \int_0^L p w(x) dx - \frac{1}{2} \int_0^L N_0 \left(\frac{dw}{dx} \right)^2 dx \end{aligned} \quad (3.3)$$

where N_0 is an external and axial compressive load. Thus, the second term is added to the original equation for capturing the shear deformation effects in Timoshenko beam theory. Furthermore, Chang *et al.* (2002) prove the original form of this equation for strain gradient theory

without higher-order stress. They used the characteristic size coefficient ($d^2/6$) instead of the nonlocal parameter and derived the potential energy density using integration by parts. The last three terms of Eq. (3.3) are also the work done by the axial load, lateral load and Von Karman effect, respectively.

Substituting Eq. (2.3) into Eq. (3.3) and integrating over the cross-sectional area, the following expression is obtained for Π

$$\begin{aligned} \Pi = & \frac{1}{2} \int_0^L \left[EA \left(\frac{du}{dx} \right)^2 + EI \left(\frac{d\phi}{dx} \right)^2 + K_S GA \left(\frac{dw}{dx} + \phi \right)^2 \right] dx \\ & - \frac{1}{2} (e_0 a)^2 \int_0^L \left[EA \left(\frac{d^2 u}{dx^2} \right)^2 + EI \left(\frac{d^2 \phi}{dx^2} \right)^2 + K_S GA \left(\frac{d^2 w}{dx^2} + \frac{d\phi}{dx} \right)^2 \right] dx \\ & + \int_0^L \left(N_0 \frac{du}{dx} \right) dx - \int_0^L p w(x) dx - \frac{1}{2} \int_0^L N_0 \left(\frac{dw}{dx} \right)^2 dx \end{aligned} \quad (3.4)$$

4. Governing differential equations and boundary conditions

The classical axial force N_{CL} acting on the beam cross-section is defined as

$$N_{CL} = EA \frac{du}{dx} \quad (4.1)$$

Using the above expression for N_{CL} and ignoring the laterally distributed loads p for buckling analysis, the variation of Eq. (3.4) with respect to $u(x)$ and equating to zero, it can be written as

$$\delta_u(\Pi) = \int_0^L \left[N_{CL} \frac{d\delta u}{dx} - (e_0 a)^2 \left(\frac{dN_{CL}}{dx} \right) \frac{d^2 \delta u}{dx^2} + N_0 \frac{d\delta u}{dx} \right] dx = 0 \quad (4.2)$$

Integrating by parts, we get

$$\begin{aligned} \delta_u(\Pi) = & [N_{CL} \delta u]_{x=0}^{x=L} - \int_0^L \left[\frac{dN_{CL}}{dx} \delta u \right] dx - \left[(e_0 a)^2 \left(\frac{dN_{CL}}{dx} \right) \frac{d\delta u}{dx} \right]_{x=0}^{x=L} \\ & + \int_0^L \left[(e_0 a)^2 \left(\frac{d^2 N_{CL}}{dx^2} \right) \frac{d\delta u}{dx} \right] dx + [N_0 \delta u]_{x=0}^{x=L} - \int_0^L \left[\frac{dN_0}{dx} \delta u \right] dx = 0 \end{aligned} \quad (4.3)$$

Integrating by parts again, we obtain

$$\begin{aligned} \delta_u(\Pi) = & [N_{CL} \delta u]_{x=0}^{x=L} - \int_0^L \left[\frac{d}{dx} N_{CL} \delta u \right] dx - \left[(e_0 a)^2 \left(\frac{dN_{CL}}{dx} \right) \frac{d\delta u}{dx} \right]_{x=0}^{x=L} \\ & + \left[(e_0 a)^2 \left(\frac{d^2 N_{CL}}{dx^2} \right) \delta u \right]_{x=0}^{x=L} - \int_0^L \left[(e_0 a)^2 \left(\frac{d^3 N_{CL}}{dx^3} \right) \delta u \right] dx \\ & + [N_0 \delta u]_{x=0}^{x=L} - \int_0^L \left[\frac{dN_0}{dx} \delta u \right] dx = 0 \end{aligned} \quad (4.4)$$

Assuming the strain gradient approach in Eq. (3.2)₁ for the nonlocal axial force N_{NL} and by some simplification, we obtain

$$\begin{aligned} \delta_u(\Pi) &= \left[N_{CL} + (e_0a)^2 \left(\frac{d^2 N_{CL}}{dx^2} \right) + N_0 \right] \delta u \Big|_{x=0}^{x=L} \\ &\quad - \int_0^L \left[\frac{dN_{CL}}{dx} + (e_0a)^2 \left(\frac{d^3 N_{CL}}{dx^3} \right) + \frac{dN_0}{dx} \right] \delta u \, dx - \left[(e_0a)^2 \left(\frac{dN_{CL}}{dx} \right) \frac{d\delta u}{dx} \right]_{x=0}^{x=L} \\ &= (N_{NL} + N_0) \delta u \Big|_{x=0}^{x=L} - \left[(e_0a)^2 \left(\frac{dN_{CL}}{dx} \right) \frac{d\delta u}{dx} \right]_{x=0}^{x=L} - \int_0^L \left[\frac{dN_{NL}}{dx} + \frac{dN_0}{dx} \right] \delta u \, dx = 0 \end{aligned} \quad (4.5)$$

Thus, the governing equation and boundary conditions in the x direction are derived from Eqs. (4.2)-(4.5), as follows

$$\begin{aligned} \frac{d}{dx}(N_{NL} + N_0) &= 0 & (N_{NL} + N_0) \delta u \Big|_{x=0}^{x=L} &= 0 \\ - (e_0a)^2 \left(\frac{dN_{CL}}{dx} \right) \delta \frac{du}{dx} \Big|_{x=0}^{x=L} &= 0 \end{aligned} \quad (4.6)$$

Performing variation with respect to $w(x)$ for Eq. (3.4) and equating to zero, it gives

$$\begin{aligned} \delta_w(\Pi) &= \int_0^L \left[K_S GA \left(\frac{dw}{dx} + \phi \right) \frac{d\delta w}{dx} - (e_0a)^2 K_S GA \left(\frac{d^2 w}{dx^2} + \frac{d\phi}{dx} \right) \frac{d^2 \delta w}{dx^2} \right] dx \\ &\quad - \int_0^L \left(N_0 \frac{dw}{dx} \frac{d\delta w}{dx} \right) dx = 0 \end{aligned} \quad (4.7)$$

Integrating by parts, we obtain the governing equation and boundary conditions for w as

$$\begin{aligned} \frac{dQ_{NL}}{dx} &= N_0 \frac{d^2 w}{dx^2} & \left[Q_{NL} - N_0 \frac{dw}{dx} \right] \delta w \Big|_0^L &= 0 \\ \left[-(e_0a)^2 K_S GA \left(\frac{d^2 w}{dx^2} + \frac{d\phi}{dx} \right) \right] \frac{d\delta w}{dx} \Big|_0^L &= 0 \end{aligned} \quad (4.8)$$

In the same way, applying the variational operator to $\phi(x)$ for Eq. (3.4) and equating to zero, we obtain

$$\begin{aligned} \delta_\phi(\Pi) &= \int_0^L \left[\left(EI \frac{d\phi}{dx} \right) \frac{d\delta\phi}{dx} - \left((e_0a)^2 EI \frac{d^2 \phi}{dx^2} \right) \frac{d^2 \delta\phi}{dx^2} + K_S GA \left(\frac{dw}{dx} + \phi \right) \delta\phi \right] dx \\ &\quad - \int_0^L \left[(e_0a)^2 K_S GA \left(\frac{d^2 w}{dx^2} + \frac{d\phi}{dx} \right) \frac{d\delta\phi}{dx} \right] dx = 0 \end{aligned} \quad (4.9)$$

Using integration by parts, the governing equation is given by

$$\frac{dM_{NL}}{dx} = Q_{NL} \quad (4.10)$$

and the following boundary conditions are derived

$$\left[M_{NL} - (e_0a)^2 K_S GA \left(\frac{d^2 w}{dx^2} + \frac{d\phi}{dx} \right) \right] \delta\phi \Big|_0^L = 0 \quad \left[-(e_0a)^2 EI \frac{d^2 \phi}{dx^2} \right] \frac{d\delta\phi}{dx} \Big|_0^L = 0 \quad (4.11)$$

Substituting the nonlocal shear force and bending moment defined in Eqs. (2.5)_{2,3} into the governing Eqs. (4.8)₁ and (4.10), and omitting the similar terms from both sides of the equations, we obtain

$$\begin{aligned} K_S GA \left(\frac{d^2 w}{dx^2} + \frac{d\phi}{dx} \right) + (e_0 a)^2 N_0 \frac{d^4 w}{dx^4} &= N_0 \frac{d^2 w}{dx^2} \\ EI \frac{d^2 \phi}{dx^2} &= K_S GA \left(\frac{dw}{dx} + \phi \right) \end{aligned} \quad (4.12)$$

Solving Eq. (4.12)₁ for ϕ gives

$$\frac{d\phi}{dx} = \frac{1}{K_S GA} \left[N_0 \frac{d^2 w}{dx^2} - (e_0 a)^2 N_0 \frac{d^4 w}{dx^4} \right] - \frac{d^2 w}{dx^2} \quad (4.13)$$

By differentiating Eq. (4.12)₂ and inserting Eq. (4.13) in Eq. (4.12)₂, the transverse equilibrium equation in terms of the lateral displacement for an axially loaded beam using a nonlocal strain gradient theory is obtained as

$$\left[\frac{EI(e_0 a)^2 N_0}{K_S GA} \right] \frac{d^6 w}{dx^6} + \left[EI - \frac{EI}{K_S GA} N_0 - (e_0 a)^2 N_0 \right] \frac{d^4 w}{dx^4} + N_0 \frac{d^2 w}{dx^2} = 0 \quad (4.14)$$

where N_0 is an external axial compressive load. This equation is similar to that obtained by Reddy and Pang (2008) for buckling of the nonlocal Timoshenko beam using Hamilton's Principle.

In addition, for solving the above equation, six boundary conditions are required (three for each end) but eight boundary conditions appear in Eqs. (4.8)_{2,3} and (4.11). It means that there is one additional boundary condition for each end. So, the main objective is to select three independent boundary conditions which can satisfy all four boundary conditions for each end. In the next part, the boundary conditions for various beam supports are obtained.

The nondimensional form of Eq. (4.14) using length of the beam L , as a nondimensionalizing parameter can be rewritten as

$$(L^4 \bar{\mu} \bar{\Omega}) \frac{d^6 w}{dx^6} + L^2 \left(\frac{1}{\pi^2 r} - \bar{\Omega} - \bar{\mu} \right) \frac{d^4 w}{dx^4} + \frac{d^2 w}{dx^2} = 0 \quad (4.15)$$

where $\bar{\Omega}$ and $\bar{\mu}$ are the nondimensional forms of shear deformation and nonlocal parameters, respectively, and r is the ratio of the critical buckling loads as follows

$$\bar{\Omega} = \frac{EI}{K_S GA L^2} \quad \bar{\mu} = \left(\frac{e_0 a}{L} \right)^2 \quad r = \frac{N_{cr}^{NL}}{N_{cr}^L} \quad (4.16)$$

where N_{cr}^{NL} is obtained from solving the Eq. (4.14) and N_{cr}^L is that given by classic Euler columns for simply supported end conditions.

We may simply switch to nonlocal Euler-Bernoulli beam model by ignoring the shear deformation terms. Additionally, the local Timoshenko beam model is obtained by letting the nonlocal parameter to be zero and by setting the shear deformation and nonlocal parameters to zero, the local Euler-Bernoulli beam model appears.

5. Buckling solutions

Here we consider analytical solutions based on a linear polynomial plus trigonometric functions different from the purely trigonometric series, for nonlocal Timoshenko beams under a constant axial compressive load, using the buckling equation obtained in Eq. (4.14) for the clamped end

conditions. This sixth order equation exhibits different solutions depending on the ratio r , and the nonlocal and shear deformation parameters $\bar{\mu}$ and $\bar{\Omega}$. The discriminant of the characteristic equation corresponding to differential Eq. (4.14) is defined as follows

$$\Delta = \left[\frac{EI}{N_0} - \frac{EI}{K_S GA} - (e_0 a)^2 \right]^2 - 4 \left[\frac{EI(e_0 a)^2}{K_S GA} \right] = L^4 \left[\left(\frac{1}{\pi^2 r} - \bar{\Omega} - \bar{\mu} \right)^2 - 4\bar{\mu}\bar{\Omega} \right] \quad (5.1)$$

If $\Delta > 0$, one of the solutions is

$$w(x) = c_1 + c_2 x + c_3 \sin(Px) + c_4 \cos(Px) + c_5 \sin(Qx) + c_6 \cos(Qx) \quad (5.2)$$

where c_1, c_2, \dots, c_6 are constants of integration and determined by six boundary conditions. P and Q are given by

$$P = \sqrt{\frac{\frac{EI}{N_0} - \frac{EI}{K_S GA} - (e_0 a)^2 - \sqrt{\Delta}}{2 \left[\frac{EI(e_0 a)^2}{K_S GA} \right]}} \quad Q = \sqrt{\frac{\frac{EI}{N_0} - \frac{EI}{K_S GA} - (e_0 a)^2 + \sqrt{\Delta}}{2 \left[\frac{EI(e_0 a)^2}{K_S GA} \right]}} \quad (5.3)$$

If $\Delta < 0$, the other solution is defined as

$$w(x) = c_1 + c_2 x + c_3 e^{Rx} \cos(Sx) + c_4 e^{Rx} \sin(Sx) + c_5 e^{-Rx} \cos(Sx) + c_6 e^{-Rx} \sin(Sx) \quad (5.4)$$

where R and S are

$$R = \frac{1}{2} \left\{ \frac{K_S GA}{EI(e_0 a)^2} \left[2 + \frac{\frac{EI}{K_S GA} + (e_0 a)^2 - \frac{EI}{N_0}}{e_0 a \sqrt{\frac{EI}{K_S GA}}} \right]^2 \right\}^{\frac{1}{4}} \quad (5.5)$$

$$S = \frac{1}{2} \left\{ \frac{K_S GA}{EI(e_0 a)^2} \left[2 - \frac{\frac{EI}{K_S GA} + (e_0 a)^2 - \frac{EI}{N_0}}{e_0 a \sqrt{\frac{EI}{K_S GA}}} \right]^2 \right\}^{\frac{1}{4}}$$

The first solution in Eq. (5.2) is found to be valid depending on the sign of Δ . Therefore, the second solution is not used in this research and is only stated for completeness.

5.1. Clamped beams

Regarding the classical continuum mechanics for clamped boundary conditions, the deflection and rotation of the cross-section are zero at each boundary. Thus, we use these classical as well as the newly derived boundary conditions in Eqs. (4.8)_{2,3} and (4.11) to derive the following boundary conditions. To this end, we satisfy all four boundary conditions, as defined in Eqs. (4.8)_{2,3} and (4.11) for each end

$$w = 0 \quad \frac{dw}{dx} = 0 \quad [N_0(e_0 a)^2] \frac{d^5 w}{dx^5} + (K_S GA - N_0) \frac{d^3 w}{dx^3} = 0 \quad (5.6)$$

Substituting these boundary conditions in Eq. (5.2) and setting the determinant of the coefficient matrix to be zero, the critical buckling load is derived as

$$N_{critical} = \frac{4\pi^2 L^2 EI K_S GA}{L^4 K_S GA + 4\pi^2 L^2 EI + 4\pi^2 L^2 (e_0 a)^2 K_S GA + 16\pi^4 EI (e_0 a)^2} \quad (5.7)$$

The critical buckling load using the dimensionless parameters $\bar{\mu}$ and $\bar{\Omega}$ is

$$N_{critical} = \frac{4\pi^2 EI}{L^2} \left[\frac{1}{1 + 4\pi^2(\bar{\mu} + \bar{\Omega}) + 16\pi^4(\bar{\mu}\bar{\Omega})} \right] \quad (5.8)$$

This equation may be transformed into the nonlocal Euler-Bernoulli theory, for the shear parameter set to zero, $\bar{\Omega} = 0$, or classical Timoshenko beam theory, for the nonlocal parameter set to zero, $\bar{\mu} = 0$, or classical Euler-Bernoulli beam theory, for both the shear and the nonlocal parameters set to zero, $\bar{\Omega} = \bar{\mu} = 0$.

6. Numerical results

6.1. Comparison of critical buckling loads for beam theories

In this section, we consider numerical solutions for CNTs modeled as nanobeams with circular cross sections. The numerical results are presented in the form of graphs and tables for different types of end conditions, using the following effective properties of carbon nanotubes (Reddy and Pang, 2008)

$$\begin{aligned}
 E &= 1000 \text{ GPa} & G &= 420 \text{ GPa} & d &= 1 \text{ nm} \\
 K_S &= 0.877 & I &= \frac{\pi d^4}{64} = 0.049 \text{ (nm)}^4 & A &= \frac{\pi d^2}{4} = 0.785 \text{ (nm)}^2
 \end{aligned}
 \tag{6.1}$$

A plot of the critical buckling loads for the nonlocal clamped Timoshenko beam with different values of shear deformation and nonlocal parameters is presented in Fig. 1.

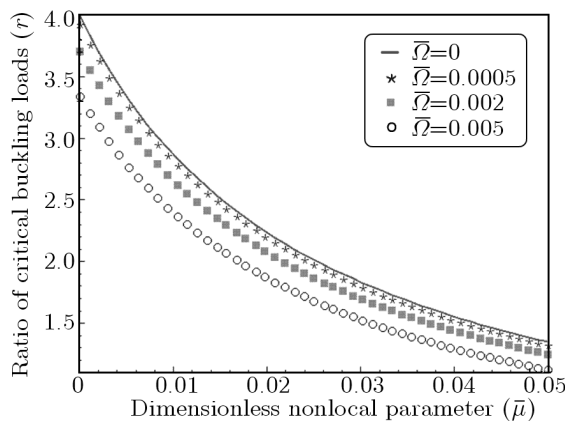


Fig. 1. Plot of the ratios of buckling loads for different values of $\bar{\mu}$ and $\bar{\Omega}$

As illustrated in Fig. 1, the solid lines for $\bar{\Omega} = 0$ denote Euler-Bernoulli beams which are the upper bound solutions. By increasing the shear deformation parameter, $\bar{\Omega}$, the critical buckling loads decrease. The effect of shear deformation is quantified for different boundary conditions. This effect is negligible for L/d ratios more than 20 (or $\bar{\Omega}$ less than 0.0005), but significant by increasing the $\bar{\Omega}$, for L/d ratios less than 20. As we are discussing about the short CNTs (i.e., $2 < L/d < 8$), this effect is visible. In fact, the shear effect is independent of $\bar{\mu}$ parameter. It is effective for deep beams in the whole analyzed range of $\bar{\mu}$.

Moreover, the intersections of the curves and the y-axes (i.e., $\bar{\mu} = 0$) are the ratios of the local critical buckling loads. Specifically, for $\bar{\Omega} = 0$, these values are the same as the local Euler-Bernoulli beam solutions.

Furthermore, the comparison of the ratio of the critical buckling loads, r , for clamped end conditions and with respect to the nonlocal Euler-Bernoulli, Timoshenko and exact Timoshenko solutions are presented in Table 1.

As it may be observed from Table 1, the first row of the table indicates the local form (i.e., $\bar{\mu} = 0$), and in this state the solution of the nonlocal Timoshenko beam without higher-order boundary conditions and exact nonlocal Timoshenko beam are the same. This is because of ignoring the nonlocal parameter that leads to ignoring the higher-order boundary conditions.

In general, the shear deformation and nonlocal parameters have the effect of reducing the buckling loads. This effect is the most significant for clamped beams (up to 7%) and the least significant for cantilever beams (about 1%).

Table 1. Comparison of the ratio of the critical buckling loads for clamped beams with respect to nonlocal Euler-Bernoulli, Timoshenko and exact Timoshenko solutions

$\bar{\Omega} = 0.00170$				$\bar{\Omega} = 0.00075$				$\bar{\Omega} = 0.00042$			
$\bar{\mu}$	NEBT	NTBT	Exact r	$\bar{\mu}$	NEBT	NTBT	Exact r	$\bar{\mu}$	NEBT	NTBT	Exact r
0	4.0000	3.7491	3.7491	0	4.0000	3.8845	3.8845	0	4.0000	3.9342	3.9342
0.0025	3.6407	3.4317	3.4123	0.0011	3.8335	3.7273	3.7228	0.0006	3.9030	3.8403	3.8389
0.0100	2.8678	2.7365	2.6880	0.0044	3.4080	3.3238	3.3096	0.0025	3.6408	3.5861	3.5808
0.0225	2.1184	2.0458	1.9855	0.0100	2.8678	2.8079	2.7850	0.0056	3.2727	3.2285	3.2188
0.0400	1.5509	1.5117	1.4536	0.0178	2.3492	2.3089	2.2813	0.0100	2.8679	2.8339	2.8207

6.2. Validation of critical buckling strains

In this subsection, the numerical results for critical buckling strains obtained from this continuum mechanics theory are compared with those obtained from MD simulations and the Sanders shell theory (Silvestre *et al.*, 2011). Since the MD simulations referenced herein consider the CNTs with fixed ends, we also consider the NTBT model with fully clamped boundary conditions. In addition, CNT(5,5) is analyzed with a diameter $d = 6.71 \text{ \AA}$ and CNT(7,7) with a diameter $d = 9.40 \text{ \AA}$, for different lengths. Both nanotubes are modeled using a thickness $h = 0.66 \text{ \AA}$, Young's modulus $E = 5.5 \text{ TPa}$ and Poisson's ratio $\nu = 0.19$ (Yakobson *et al.*, 1996). The lengths of CNTs used in the following table are extracted from the work done by Silvestre *et al.* (2011). The results from MD simulations, nonlocal Timoshenko beam and Sanders shell models are compared in Table 2.

Table 2. Comparison between critical buckling strains of CNT(5,5) and CNT(7,7) obtained from MD simulations, Sanders shell theory (SST) and proposed nonlocal Timoshenko beam theory (NTBT)

$L [\text{\AA}]$	$d [\text{\AA}]$	MD	NTBT	SST	Local buckling	Global buckling
16.09	6.71	0.08146	0.08461	0.08729	0.08779	0.85862
21.04	6.71	0.07528	0.08280	0.08288	0.08050	0.50210
28.46	6.71	0.06992	0.06964	0.07858	0.06955	0.27430
28.29	9.40	0.06514	0.06568	0.06582	0.06164	0.54467
40.59	9.40	0.04991	0.05825	0.05885	0.05384	0.26469
52.88	9.40	0.04710	0.04607	0.05600	0.04776	0.15591

It is seen that the critical buckling strains are in good agreement as compared with the results obtained from MD simulations as well as Sanders shell theory. Moreover, the results show that unlike the other beam theories, this model could capture correctly the length-dependent buckling strains of short CNTs for the mode of shell-type buckling. In fact, the available beam models are unable to show the correct trend in critical axial buckling strains of short CNTs, while the proposed nonlocal beam model shows much better agreement with the molecular dynamics simulation results.

Finally, based on the MD simulation results, the value of nonlocal constant is determined for CNTs based on an averaging process. The best match between MD simulations and nonlocal formulations is achieved for a nonlocal constant value of $e_0a = 0.3$ for CNT(5,5) and $e_0a = 0.53$ for CNT(7,7) with good accuracy (the error is less than 10%).

7. Conclusion

A nonlocal Timoshenko beam model was developed and buckling behavior of CNTs was analyzed using a mixed approach based on the strain gradient theory and variational method of total potential energy. This approach provides governing equations and variationally consistent sets of boundary conditions for various end supports.

In addition, the exact and closed-form eigenvalues of the nonlocal critical buckling loads for nanobeams with clamped end conditions were investigated, which are more complete and accurate compared with those available in the literature. These solutions could simply be reduced to the nonlocal Euler-Bernoulli, classical Timoshenko and classical Euler-Bernoulli beam models by ignoring the nondimensional shear deformation parameter $\bar{\Omega}$, nonlocal parameter $\bar{\mu}$ or both of them, respectively.

Moreover, the small-scale effects and shear deformation parameter are specifically highlighted for this model using higher-order boundary conditions. In this case, it is clearly observed that the critical buckling loads obtained from Eq. (5.8) for clamped nanobeams are always smaller than those predicted by the classical model. In fact, the nonlocal parameter $\bar{\mu}$ and shear deformation parameter $\bar{\Omega}$ have the effect of reducing the buckling load. For the short CNTs (i.e., $2 < L/d < 8$), the shear effect is visible and effective for the whole analyzed range of $\bar{\mu}$.

References

1. CHANG C.S., ASKES H., SLUYS L.J., 2002, Higher-order strain/higher-order stress gradient models derived from a discrete microstructure, with application to fracture, *Engineering Fracture Mechanics*, **69**, 1907-1924
2. ERINGEN A.C., 1972, Nonlocal polar elastic continua, *Int. J. Eng. Sci.*, **10**, 1-16
3. ERINGEN A.C., 1976, *Continuum Physics Volume IV: Polar and Nonlocal Field Theories*, Academic Press, New York
4. ERINGEN A.C., 1983, On differential equations of nonlocal elasticity and solutions of screw dislocation and surface waves, *J. Appl. Phys.*, **54**, 4703-4710
5. ERINGEN A.C., 2002, *Nonlocal Continuum Field Theories*, Springer-Verlag, New York
6. ERINGEN A.C., EDELEN D.G.B., 1972, on nonlocal elasticity, *Int. J. Eng. Sci.*, **10**, 233-248
7. FELICIANO J., TANG C., ZHANG Y., CHEN C., 2011, Aspect ratio dependent buckling mode transition in single-walled carbon nanotubes under compression, *J. Appl. Phys.*, **109**, 084323
8. IJIMA S., 1991, Helical micro tubes of graphitic carbon, *Nature*, **354**, 56-58
9. KUMAR D., HEINRICH C., WAAS A.M., 2008, Buckling analysis of carbon nanotubes modeled using nonlocal continuum theories, *J. Appl. Phys.*, **103**, 073521
10. LU P., LEE H.P., LU C., ZHANG P.Q., 2006, Dynamic properties of flexural beams using a nonlocal elasticity model, *J. Appl. Phys.*, **99**, 073510
11. MUC A., 2011, Modelling of carbon nanotubes behaviour with the use of a thin shell theory, *Journal of Theoretical and Applied Mechanics*, **49**, 2, 531-540
12. PEDDIESON J., BUCHANAN G.R., MCNITT R.P., 2003, Application of nonlocal continuum models to nanotechnology, *Int. J. Eng. Sci.*, **41**, 305-312
13. POSTMA H.W.C., TEEPEN T., YAO Z., GRIFONI M., DEKKER C., 2001, Carbon nanotube single-electron transistors at room temperature, *Science*, **293**, 5527, 76-79
14. REDDY J.N., PANG S.D., 2008, Nonlocal continuum theories of beams for the analysis of carbon nanotubes, *J. Appl. Phys.*, **103**, 023511

15. REDDY J.N., 2007, Nonlocal theories for bending, buckling and vibration of beams, *Int. J. Eng. Sci.*, **45**, 288-307
16. SEIDEL R.V., GRAHAM A.P., KRETZ J., RAJASEKHARAN B., DUESBERG G.S., LIEBAU M., UNGER E., KREUPL F., HOENLEIN W., 2005, Sub-20 nm short channel carbon nanotube transistors, *Nano Lett.*, **5**, 1, 147-50
17. SILVESTRE N., WANG C.M., ZHANG Y.Y., XIANG Y., 2011, Sanders shell model for buckling of single-walled carbon nanotubes with small aspect ratio, *Composite Structures*, **93**, 1683-1691
18. SUDAK L.J., 2003, Column buckling of multi-walled carbon nanotubes using nonlocal continuum mechanics, *J. Appl. Phys.*, **94**, 7281-7287
19. WANG B., ZHAO J., ZHAO S., 2010, A micro-scale Timoshenko beam model based on strain gradient elasticity theory, *Eur. J. Mech. A/Solids*, **29**, 591-599
20. WANG C.M., ZHANG Y.Y., HE X.Q., 2007, Vibration of nonlocal Timoshenko beams, *Nanotechnology*, **18**, 105401
21. WANG C.M., ZHANG Y.Y., XIANG Y., REDDY J.N., 2010, Recent studies on buckling of carbon nanotubes, *Appl. Mech. Rev.*, **63**, 030804
22. WANG Q., 2005, Wave propagation in carbon nanotubes via nonlocal continuum mechanics, *J. Appl. Phys.*, **98**, 124301
23. WANG Q., WANG C.M., 2007, the constitutive relation and small scale parameter of nonlocal continuum mechanics for modeling carbon nanotubes, *Nanotechnology*, **18**, 075702
24. WANG Q., VARADAN V.K., QUEK S.T., 2006, Small scale effect on elastic buckling of carbon nanotubes with nonlocal continuum models, *Phys. Lett. A*, **357**, 130-135
25. WANG Y.Z., LI F.M., KISHIMOTO K., 2010, Scale effects on thermal buckling properties of carbon nanotube, *Physics Letters A*, **374**, 4890-4893
26. YAKOBSON B.I., BRABEC C.J., BERNHOLC J., 1996, Nanomechanics of carbon tubes: instabilities beyond linear response, *Phys Rev Lett.*, **76**, 2511-2514
27. YANG J., KE L.L., KITIPORNCHAI S., 2010, Nonlinear free vibration of single-walled carbon nanotubes using nonlocal Timoshenko beam theory, *Physica E*, **42**, 1727-1735
28. ZHANG Y.Y., WANG C.M., DUAN W.H., XIANG Y., ZONG Z., 2009, Assessment of continuum mechanics models in predicting buckling strains of single-walled carbon nanotubes, *Nanotechnology*, **20**, 395707
29. ZHANG Y.Q., LIU G.R., WANG J.S., 2004, Small-scale effects on buckling of multi-walled carbon nanotubes under axial compression, *Phys. Rev. B*, **70**, 205430

Analiza wyboczenia krótkich nanorurek węglowych na podstawie zmodyfikowanego modelu belki Timoszenki

Streszczenie

W pracy zaprezentowano nową metodę analizy problemu wyboczenia krótkich, obustronnie zamurowanych nanorurek węglowych (tzw. CTN – *Carbon NanoTubes*) z uwzględnieniem zjawisk małoskalowych. Na podstawie nielokalnego sformułowania kinematyki belki Timoszenki opracowano teorię gradientu odkształcenia oraz metodę analizy wariacyjnej, wyprowadzono równania konstytutywne wyższego rzędu i odpowiadające im warunki brzegowe, do tej pory z rzadka stosowane w tego typu zagadnieniach. Następnie rozwiązano równania modelu, z których wyznaczono dokładną wartość krytycznego obciążenia

prowadzącego do wyboczenia. Użyto w tym celu kombinacji funkcji wielomianowych i trygonometrycznych zamiast szeregów wyłącznie trygonometrycznych. Zbadano również wpływ współczynników skali, proporcji oraz odkształcenia postaciowego na wyboczenie utwierdzonych nanorurek CNT. W trakcie symulacji numerycznych dynamiki molekularnej modelu wykazano dobrą zbieżność otrzymanych wyników z powłokowym modelem Sandersa. Potwierdzono, że – w odróżnieniu od innych teorii belek – zastosowany model dokładnie odzwierciedla efekty małoskalowe przy opisie powłokowego wyboczenia krótkich nanorurek CNT.

Manuscript received September 12, 2011; accepted for print January 2, 2012